Computer Networks 108 (2016) 108–119

Contents lists available at ScienceDirect

Computer Networks

journal homepage: www.elsevier.com/locate/comnet

Integration of Markov random field with Markov chain for efficient event detection using wireless sensor network

Xianda Chen, Kyung Tae Kim, Hee Yong Youn*

College of Information and Communication Engineering, Sungkyunkwan University, Suwon, Korea

ARTICLE INFO

Article history:
Received 21 November 2015
Revised 12 June 2016
Accepted 11 July 2016
Available online 12 July 2016

Keywords:
Wireless sensor network
Event detection
Spatio-temporal correlation
Markov random field
Markov chain
Hierarchical model

ABSTRACT

Event detection is an important task required in various applications of wireless sensor network (WSN). The existing approaches consider the spatial and temporal correlation of sensor data separately or not in a cohesive way. In this paper an event detection scheme with WSN is introduced, which adopts a hierarchical structure to efficiently integrate the spatial and temporal correlation of sensor data. Here a fusion algorithm considering both the weight of the sensors and spatial information is applied to Markov random field to properly fuse the decisions of the neighboring nodes. Markov chain is also adopted to effectively extract the temporal correlation after the spatial correlation is decided. The simulation results demonstrate that the proposed scheme can effectively increase the detection accuracy and reduce communication cost, in comparison with the existing schemes.

1. Introduction

Consisting of spatially distributed sensor nodes, wireless sensor network (WSN) can remotely monitor the target area for temperature, sound, pressure, etc. Here the nodes cooperatively transfer the sensed data to the main server through the wireless network [1]. The number of sensor nodes in a WSN varies from a few to several hundreds or even thousands, each of which is connected to one or more sensor nodes. Each sensor node typically comprises several components: radio transceiver with internal antenna; electronic circuit and microcontroller interfacing with the sensors; energy source which is usually a battery or an embedded form of energy harvesting. The topology of WSN can vary from a simple star network to a complicated multi-hop wireless mesh network. If a complicated topology is employed, the data propagation path needs to be carefully decided considering several factors.

Event detection is one of the key applications of WSN. An event is a significant occurrence which is irregular compared to the normal patterns of the behavior of the target system. It could be a natural phenomenon or produced as a specific outcome in response to user interaction. In real world abnormal event occurs in rare occasions, and it is usually very harmful. Such events thus need instantaneous detection and reaction. For efficient event detection, WSN is deployed over a region which needs to be monitored. Fig. 1 shows the clustered organization of WSN employed for event detection. When an event occurs, each node in its vicinity sends its reading (the sensed data) to the cluster-head which performs data aggregation and forwards the data to the base station. For instance, sensor nodes could be deployed in the forest to detect fire by sensing the temperature or smoke of the fire. Early detection of fire is crucial to minimize the damage, and WSN allows quick identification of the starting position and the path of the spread of the fire.

In reality, the sensors near the place where an event occurs are likely to have similar readings since they are usually deployed with high density, which represents the spatial relationship. The sensor readings also have temporal relationship as the data are collected over a period of time [2]. Both the spatial relationship and temporal relationship are very critical for accurate event detection since the spatio-temporal correlation between the sensor readings can effectively deal with the inherent uncertainty of sensor data. Fig. 2 shows an example of spatial and temporal correlation of sensor readings, where three sensor nodes are used to monitor the temperature of a region during a period of time. Observe from the figure that the spatial correlation of the temperature value of node_*A* and node_*B* is quite high since they are close to each other. In addition, the temperatures collected by node_*A* show high temporal correlation during the time period from 9 to 19 as the values are stable in this period. The same observation is made with node_*B*. Most existing works on event detection with WSN make an inference based on only either spatial or temporal relationship. Note, however, that the changes in sensor readings caused by an event usually exhibit strong spatio-temporal correlation, while

* Corresponding author.
E-mail addresses: chenxianda0319@gmail.com, chenxianda@skku.edu (X. Chen), kyungtaekim76@gmail.com (K.T. Kim), youn7147@skku.edu (H.Y. Youn).

http://dx.doi.org/10.1016/j.comnet.2016.07.004
1389-1286/

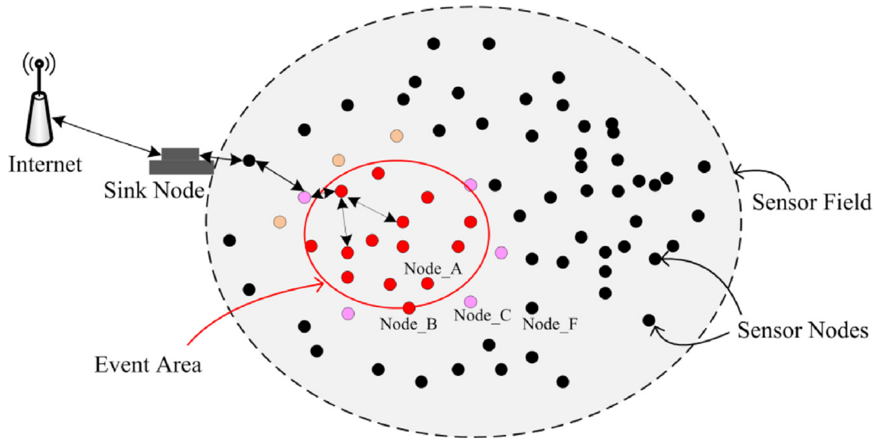

Fig. 1. Event detection with WSN.

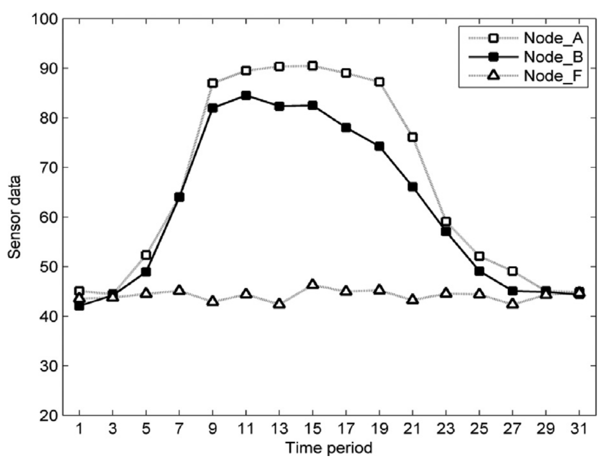

Fig. 2. An example of sensor reading.

efficiently integrating the spatial and temporal relationship is still a big challenge.

A learning-based approach [3,4] was applied for the task of event detection with WSN, where Markov random field (MRF) was employed. In addition, various event detection approaches have been proposed either based on the threshold [5–8] with or without fuzzy logic and pattern matching technique [9–14]. In the existing approaches, however, the spatial and temporal correlation of sensor data are not treated in a cohesive way. As a result, the effectiveness and accuracy of event detection cannot be maximized. In this paper, thus, we introduce a novel event detection scheme adopting a hierarchical structure to efficiently integrate the spatial and temporal correlation. Moreover, a new fusion algorithm is employed with the MRF to properly fuse the readings of neighboring sensors considering the weight of the sensors and spatial information. Markov chain is also adopted to effectively extract the temporal correlation after the spatial correlation is decided. The simulation results demonstrate that the proposed scheme effectively increases the detection accuracy and reduces the communication cost in comparison with the existing schemes. The novelty of the proposed scheme is with the new approach of MRF applied to one hop neighbor nodes and mitigation of the influence of malfunctioning sensor and noise in the temporal process.

The rest of the paper is organized as follows. Section 2 describes the related work. The hierarchical structure effectively integrating the spatial and temporal model and the fusion operation employed in the proposed scheme are presented in Section 3. Section 4 presents the results of the performance evaluation of the proposed scheme including the comparison with the existing schemes, followed by the conclusion in Section 5.

2. Related work

Event detection is one of the most important tasks of WSN. Therefore, a variety of techniques have been proposed for efficient event detection which can be classified as threshold-based, pattern-based, and learning-based.

Threshold-based approach. This is the most basic one where the events are detected based on the preset threshold value. In general, the threshold value is defined by domain expert, and the occurrence of an event is notified when the sensed value is above or below the threshold value. Simplicity is the main advantage of this approach since raw data can be directly handled inside the sensor node. A data-centric service middleware (DSWare) [5] uses a database-like abstraction to tailor the sensor network for event detection. It uses SQL-like statements for the registration and cancellation of an event. DSWare defines a compound event specification, which consists of maximum detection range, time interval, and confidence function. The confidence function describes how the different measurements collected by the sensor nodes in the monitored area are weighted and how the composition of the data is achieved. If the final value exceeds a certain threshold, a significant event is assumed to happen and then reported to the base station. The SQL-like implementation provides the flexibility and expressiveness in covering a large number of possible event specifications.

Fuzzy logic has also been used to improve the decision-making process with WSN, reducing resource consumption and increasing performance [6–8]. Note that using only crisp values cannot adequately handle imprecise sensor readings occurring often. Different from the event description based on precise value, Kapitanova et al. [8] proposed a variant event detection approach using fuzzy values instead of crisp values, which significantly improves the accuracy of event detection. This approach is useful in modeling the rate of incorrect reading of the sensors and aggregating local decisions of multiple sensors measuring the same type of data. However, it requires a considerable amount of memory for storing the rules, which is not feasible with resource constrained WSN.

Pattern-based approach. In most event detection schemes with WSN raw data are transmitted to an external entity for evaluation, causing either high communication overhead or low event detection accuracy, especially for complex events. The event detection approach based on pattern matching has been explored recently to address this issue [9–14]. [11] integrated the pattern-based approach with an in-network sensor query processing framework. Different from the existing threshold-based event detection approach, it abstracts the events into patterns in sensory data and converts the problem of event detection into a pattern matching problem. [12] used contour map as a mathematical tool to model the patterns of events. The approach includes in-network contour mapping and server-side contour map matching.

Wittenburg et al. [13] presented a system for distributed event detection, which particularly suits the specific characteristics of WSN. It employs distributed sampling of sensor nodes to maximize the accuracy of the event detection process. Different algorithms for distributing, classifying, and fusing "fingerprints" of raw data sampled by each sensor were also proposed and quantitatively evaluated in a small-scale experiment. In addition, the approach in [14] handles event and outlier detection together which are usually dealt separately in the traditional schemes. By considering the events as some sorts of outliers, the approach investigates the applicability and suitability of the techniques of pattern-matching for outlier detection.

Learning-based approach. Various machine learning techniques have also been used to decide whether an event has occurred or not. [15] proposed an ensemble distributed machine learning approach for event detection in two phases, base phase and meta phase. It detects events in a distributed manner using Support Vector Machine (SVM) classification with polynomial kernel. Since sensor nodes are deployed usually in high density, the nearby sensors are likely to have similar readings. Recently, MRF has been adopted to model the spatial relationship of neighboring nodes and perform inference about the events. In [16] a learning-based approach was proposed which uses MRF to model spatial context and stochastic interaction among observable quantities. The effectiveness of the approach was demonstrated with various practical problems, including the analysis and interpretation of medical images and remotely sensed images. The approach, however, relies on some assumptions on the observations in order to ensure computational tractability. In contrast, the conditional random field (CRF), one notable variant of MRF, relaxes the assumptions by directly modeling the conditional distribution over the hidden states given the observations. [17] presented a unified framework to capture the spatio-temporal dependencies among the observations and events using CRF.

Most existing schemes on event detection employ the inference in the spatial or temporal dimension separately. However, the changes in sensor readings caused by an event usually exhibit strong spatio-temporal correlation [18]. The spatial and temporal relationship are critical factors of accurate event detection. An effective event detection approach is proposed in this paper, which models the spatio-temporal behavior of dynamic field in an integrated way.

3. The proposed scheme

The hierarchical WSN employed in the proposed scheme is composed of spatial layer, temporal layer, and sink layer as shown in Fig. 3. In the spatial layer, a fusion function is employed to aggregate the readings of neighboring sensor nodes. The hierarchical structure allows dual layer summaries of sensor readings such as spatial summarization and temporal summarization.

3.1. Hierarchical spatio-temporal model

Fig. 3 illustrates the overall structure of spatio-temporal model employed in the proposed scheme. With such hierarchical structure, it is effective to integrate the relationship of spatial and temporal attribute.

3.1.1. Spatial layer

A synchronized WSN consisting of n sensor nodes is assumed to be able to observe the condition of the environment at nearly equal time duration. It is denoted by a set, $S = \{s_1, s_2, \dots, s_n\}$, where s_i is i-th sensor. The spatial layer is the lowest layer, which is responsible for spatial event detection using the sensors based on MRF. It models the spatial relationship and performs inference on the event in the spatial dimension. In this layer each node communicates with its immediate neighboring nodes. The radius of the communication range of each node is defined as ρ. If an event is detected by a node, marked as ***S_node***, a fusion function is used to fuse the readings of all the neighboring nodes, and the information on the event is passed to the temporal layer.

3.1.2. Temporal layer

The temporal layer is the middle layer between the spatial and sink layer, which is in charge of the processing of temporal event detection in time dimension by employing Markov chain. Markov chain is used to model the temporal relationship of the sensor readings and predict the values of sensor reading. Here only the ***S_nodes*** identified from the spatial layer are included in the Markov chain process. The node in the temporal layer is marked as ***ST_node*** if it detects a temporal event and reports it to the sink node. Other nodes in this layer do not send any data. In summary, the proposed spatio-temporal detection process involves two steps:

Step 1: MRF is adopted to model the relationship of the sensor readings and perform inference on the event in the spatial layer.

Step 2: Markov chain is used to model the relationship of the readings of ***S_nodes*** and perform inference based on the temporal evidences in the temporal layer.

3.2. Operation of event detection

There are two main operations handled in the proposed scheme: the spatial summarization and temporal summarization. The sensor readings are modeled by MRF in the spatial layer, and a spatial event is decided considering the readings of neighborhood nodes. It is then reported to the nodes of temporal layer by ***S_nodes***. Markov chain is applied to the ***S_nodes*** reporting spatial event for the inference of temporal event.

3.2.1. Spatial summarization

Let S denote a finite set of sensor nodes in the field, which means that S includes all nodes in the monitored area. For node_i ($i \in S$), a finite set of nodes are assumed to lie inside the area of the communication range (ρ) of node_i. The nodes in S are related to each other via a neighborhood system, N, which is defined as

$$N = \{N_i | \forall i \in S\} \tag{1}$$

where N_i is the set of neighbor nodes of node_i. There are two main properties for the neighbor relationship: a node is not a neighbor to itself, that is, $i \notin N_i$; and the neighbor relationship is mutual, that is, $i \in N_j$ ($\Leftrightarrow$) $j \in N_i$.

For a randomly deployed S, the set of neighbors of node_i is defined as the set of nodes within a radius of ρ from node_i.

$$N_i = \{ j \in S | Dist(node\_j, node\_i) \le \rho, j \ne i\} \tag{2}$$

where *Dist* is the Euclidean distance between any two nodes. The local conditional distribution can then be given as follows:

$$P\left(X_i = x_i | X_j = x_j, j \ne i, j \in S\right) = P\left(X_i = x_i | X_j = x_j, j \in N_i\right) \tag{3}$$

where X_i is random variable denoting node_i and x_i is a particular realization of X_i. Thereby, the random vector $\boldsymbol{X} = \{X_i\}_{i \in S}$ is a random field on the monitored area covered by S.

The sensor observation of the field S, O, is defined as Eq. (4), and the noise model added to the observation of sensor_i, o_i, is

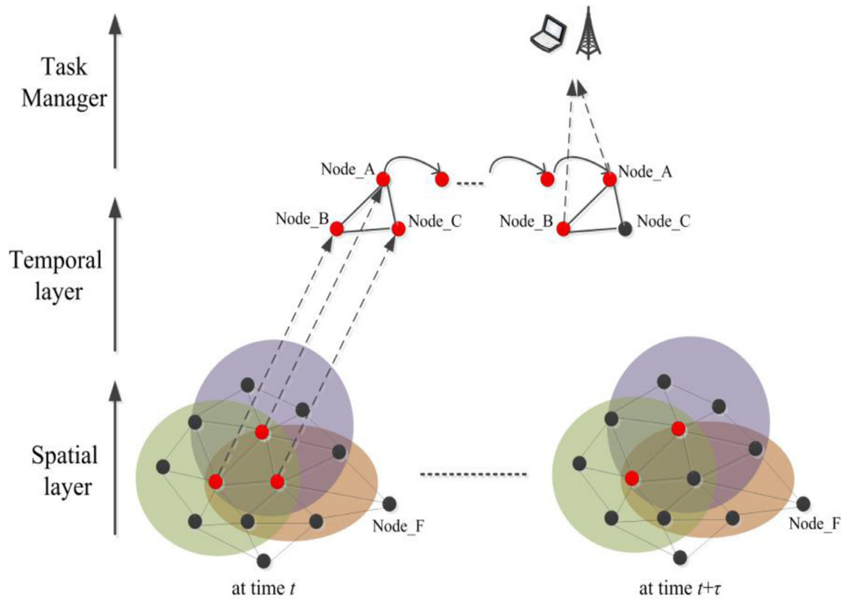

Fig. 3. The proposed hierarchical model.

given by Eq. (5). Note that the sensor observation O is the realization of the aforementioned random field $\boldsymbol{X}$, and o_i is actually the realization of the random variable X_i, that is x_i. O and o_i are used for the rest of the paper if not causing ambiguity.

$$O = \{o_i\}_{i\in S} \tag{4}$$

$$o_i = \psi_i + G_i, \ \ for\ all\ i \in S \tag{5}$$

where ψ_i is the signal strength at sensor node_i and G_i is its measured noise, assumed to be a Gaussian random variable.

The reading of nearby sensor nodes may present high spatial correlation due to the proximity. Each sensor node is designed to distinguish the false hypothesis, F, corresponding to no event and the alternative hypothesis, T, corresponding to event occurrence at its location. The *a priori* probability of both the hypotheses are denoted by P_F and P_T, respectively. Let H be the random field of the hypothesis for the field S, and $H=\{h_i\}_{i\in S}$ be a hypothesis configuration of H, where $h_i\in\{F,T\}$.

The hypothesis configuration H is fixed during the binary decision making process since the considered events of the sensor field S are assumed to be static. Each node in S observes its own hypothesis phenomenon which could be different from those observed by other nodes. Let $\phi=\{\phi_i\}_{i\in S}$ represent the decisions of all sensor nodes in S, where the decision made by node_i is denoted by Eq. (6). The binary decisions are exchanged between neighboring nodes, which are assumed to be independent.

$$\phi_i = \begin{cases} 1, & if\ F\ is\ rejected \\ 0, & otherwise \end{cases} \tag{6}$$

The spatial layer is to determine the most likely events of the sensor field, i.e. the hypothesis configuration with the highest probability. By Bayes' theorem, the probability of a hypothesis configuration given the observation can be obtained by Eq. (7), where $P(O)$ is a constant observed by the local decisions, $P(O|H)$ is the likelihood probability, and $P(H)$ is the prior probability.

$$P(H|O) = \frac{P(O|H)P(H)}{P(O)} \propto P(O|H)P(H) \tag{7}$$

As stated previously, observation O is assumed to be a Gaussian random variable, with noise added. Assume o_i is conditionally independent of all H_i, i.e.,

$$P(o_i|H) = \prod P(o_i|h_i) \tag{8}$$

And also assume that o_i is conditionally independent of each other, i.e.,

$$P(O|H) = \prod P(o_i|H) \tag{9}$$

Therefore, $P(O|H)$ can be obtained by Eq. (10), where $P(O_i|H_i)$ is represented by a Gaussian distribution with mean, μ_H, calculated by Eq. (11), and variance, $\delta^2{}_H$, calculated by Eq. (12).

$$\begin{aligned} P(O|H) &= \prod P(o_i|h_i) \\ &= \prod \frac{1}{\sqrt{2\pi\sigma_{h_i}^2}} \exp\left(-\frac{\left(o_i-\mu_{h_i}\right)^2}{2\sigma_{h_i}^2}\right) \end{aligned} \tag{10}$$

$$\mu_{h_i} = \frac{1}{\left|S_{h_i}\right|}\sum_{S_{h_i}} o_i \tag{11}$$

$$\sigma_{h_i}^2 = \frac{1}{\left|S_{h_i}\right|}\sum_{S_{h_i}} \left(o_i-\mu_{h_i}\right)^2 \tag{12}$$

The MRF model is used to decide $P(H)$ by processing the spatial summarization. An MRF is a conditional probability distribution used for analyzing the spatial dependencies of physical phenomena [19]. The MRF model is based on a set of *cliques*. A clique C is defined as a subset of nodes of S, where each node is a neighbor of all other nodes in C. For the first-order neighborhood system, C can be of a single node clique which is denoted as C_1, pair-node clique denoted as C_2, and triple-node clique denoted as C_3, etc. Then the collection of all the cliques for the kth-order neighborhood system on S is

$$C = C_1 \cup C_2 \cup C_3 \cup \cdots \cup C_k \tag{13}$$

Fig. 4 shows an example of a randomly deployed WSN and the neighborhood of a node and its cliques. The neighborhood area of node_i is marked by shaded circle.

The spatial summarization layer uses the MRF model to identify the hypothesis configuration H given the sensor observations O. For an MRF, the probability of the field configuration H can be given by

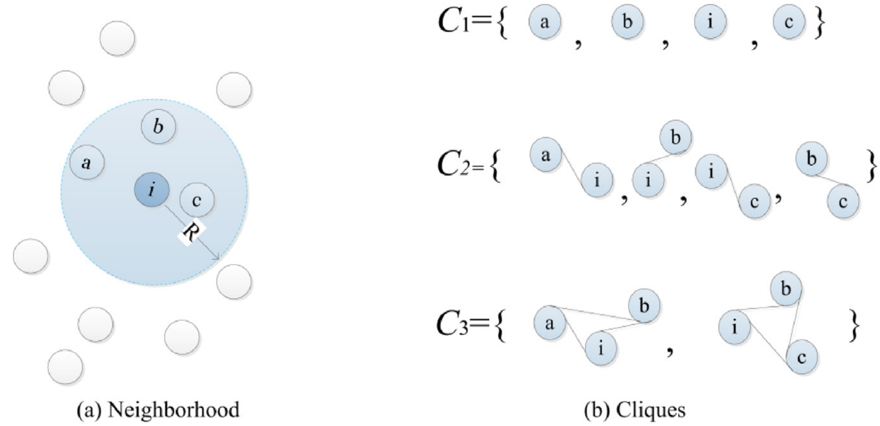

Fig. 4. An example of neighborhood system and its cliques in WSN.

a Gibbs distribution [20] shown as Eq. (14).

$$P(H=h) = Z^{-1}\mathrm{e}^{-E(h)} \tag{14}$$

where the *partition function* Z, defined as Eq. (15), is a normalization constant involving the summation over all possible configurations of H, and $E(h)$ is the energy function on h defined as Eq. (16). The energy associated with different orders of cliques are examined and summed up to yield the energy function.

$$\mathrm{Z} = \sum_{h \in H} e^{-E(h)} \tag{15}$$

$$E(h) = \sum_{\{i\}\in C} \alpha_{h_i} - \sum_{\{i\}\in C} \beta\zeta(h_i) - \sum_{\{i,j\}\in C} \delta\xi\left(h_j, h_i\right) \tag{16}$$

The parameter α_h is a cost parameter for hypothesis $h\in\{F,T\}$, which is usually set to zero for every node if the *a priori* information about the relative size of the various hypotheses is unknown [3]. Here α_h is set to 0. β is a coefficient determining the granularity of energy for single-node cliques and δ can be viewed as the spatial coefficient in the field *S*. β and δ are set to 1 in the evaluation. Data constraint $\zeta(h_i)$ shown as Eq. (17) determines the influence to the energy function exerted by the singleton clique, while smoothness constraint $\xi(h_j,h_i)$ obtained by Eq. (18) represents the influence of the neighbor nodes. $\zeta(h_i)$ reflects the observation of each node and $\xi(h_j,h_i)$ reflects the spatial consistency (the nodes close to each other are most likely have similar events).

$$\zeta(h_i) = \log\left(P(o_i|h_i)\right) \tag{17}$$

$$\xi\left(h_j, h_i\right) = \begin{cases} -1, & \text{if } h_j = h_i \\ 1, & \text{if } h_j \neq h_i \end{cases} \tag{18}$$

Due to the randomness of sensor noise and channel jitter, the binary decisions received by a node from its neighbors could vary, whereby the energy model of Eq. (16) taking all neighbors into account is not appropriate. The proposed scheme thus uses a probability function to measure the reliability of the decision of the neighbors of each node. The energy function used in the proposed scheme is then defined as Eq. (19), where e_{ji} is the reliability of the decision made by neighbor node_*j* of node_*i*, evolved from the fusion rule in [21].

$$E(h) = \sum_{\{i\}\in C} \alpha_{h_i} - \sum_{\{i\}\in C} \beta\zeta(h_i) - \sum_{\{i,j\}\in C} \delta e_{ji}\xi\left(h_j, h_i\right) \tag{19}$$

The fusion function considers both the spatial readings and binary decisions of the neighbor nodes residing inside the area of communication range of a node. The fusion function involves a two-step process. Firstly, each sensor individually performs a likelihood ratio test without communicating with each other. In the second step, each sensor performs the fusion process iteratively. Through the fusion rule, node_*i* produces an updated decision, e_{ji}, considering its observation, o_i, and the received binary decisions $\{\phi_{ji}\}_{j\in Ns}$, where ϕ_{ji} is the binary decision received by node_*i* from neighbor node_*j*. The fusion rule can be expressed by Eq. (20).

$$e_{ji} = \begin{cases} 1, & \dfrac{P(h_i = T|o_i, \{\phi_{ji}\}_{j\in N_i})}{P(h_i = F|o_i, \{\phi_{ji}\}_{j\in N_i})} \geq 1 \\ 0, & \dfrac{P(h_i = T|o_i, \{\phi_{ji}\}_{j\in N_i})}{P(h_i = F|o_i, \{\phi_{ji}\}_{j\in N_i})} < 1 \end{cases} \tag{20}$$

By Bayes' theorem, Eq. (20) can be rewritten in the form of a likelihood ratio test as Eq. (21).

$$e_{ji} = \begin{cases} 1, \Lambda\left(o_i, \left\{\phi_{ji}\right\}_{j\in N_i}\right) \geq \eta \\ 0, \Lambda\left(o_i, \left\{\phi_{ji}\right\}_{j\in N_i}\right) < \eta \end{cases} \tag{21}$$

$$\Lambda\left(o_i, \left\{\phi_{ji}\right\}_{j\in N_i}\right) = \frac{P\left(o_i, \left\{\phi_{ji}\right\}_{j\in N_i}|h_i = T\right)}{P\left(o_i, \left\{\phi_{ji}\right\}_{j\in N_i}|h_i = F\right)} \tag{22}$$

where $\eta = P_F/P_T$. The fusion rule, e_{ji}, is used to successively update the decision of the sensor node by taking the new observation and binary decisions received from the neighboring nodes into account. It determines how the neighbors influence the energy of the field shown in Eq. (19).

3.2.2. Example of spatial summarization

An example of sensor field with four nodes is used to explain the proposed scheme of spatial summarization. As shown in Fig. 5, assume the observations of {80, 77, 57, 67} in the nodes with the threshold of 70. Therefore, the hypothesis phenomena of the field are {*T, T, F, F*}. The spatial layer is to determine the hypothesis configuration H with the highest probability given the sensor observations O. The following steps show the procedure for getting the probability $P(H|O)$, assuming $H = \{1, 0, 0, 1\}$.

First, $P(O|H)$ is Obtained.

$$H = \{1, 0, 0, 1\};\ O = \{80, 77, 57, 67\}$$

$$\mu_{H=0} = \frac{1}{|S_{H=0}|}\sum_{i\in S_{H=0}} o_i = \frac{1}{2}(77+57) = 67;\ \mu_{H=1} = 73.5$$

$$\sigma^2_{H=0} = \frac{1}{|S_{H=0}|}\sum_{i\in S_{H=0}} (o_i - \mu_{H=0})^2 = 100;\ \sigma^2_{H=1} = 42.25$$

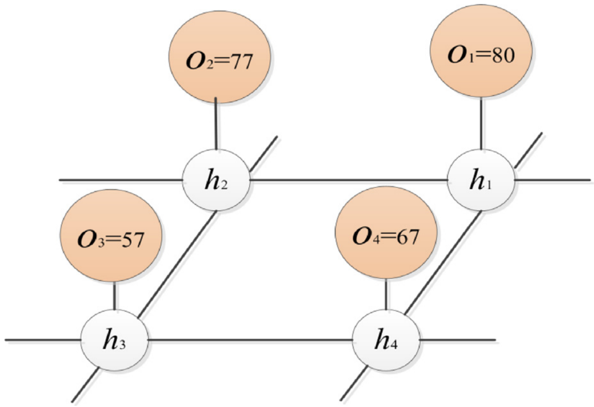

Fig. 5. A case study of spatial summarization.

Table 1
$P(H|O)$ for all hypothesis configurations.

h_1	h_2	h_3	h_4	$P(O\|H)$	$E(H)$	$P(H)$	$P(H\|O)$
0	0	0	0	2.80489E−5	0.552084	0.087704	2.46002E−6
0	0	0	1	1.06651E−4	5.972036	0.000388	4.14125E−8
0	0	1	0	6.61610E−4	5.179398	0.000857	5.67555E−7
0	0	1	1	3.33005E−3	6.477549	0.000234	7.79969E−7
0	1	0	0	1.35852E−4	1.866933	0.023550	3.19932E−6
0	1	0	1	5.66636E−5	8.246696	0.000039	2.26256E−9
0	1	1	0	4.43417E−5	4.353187	0.001959	8.69037E−8
0	1	1	1	2.08552E−4	5.680786	0.000519	1.08360E−7
1	0	0	0	2.08552E−4	1.680786	0.028368	5.91627E−6
1	0	0	1	4.43417E−5	4.353187	0.001959	8.69037E−8
1	0	1	0	5.66636E−5	8.246696	0.000039	2.26256E−9
1	0	1	1	1.35852E−4	5.866933	0.000431	5.85975E−8
1	1	0	0	3.33005E−3	-1.52245	0.698204	2.32505E−3
1	1	0	1	6.61610E−4	1.179398	0.046836	3.09875E−5
1	1	1	0	1.06651E−4	1.972036	0.021200	2.26105E−6
1	1	1	1	2.80489E−5	0.552084	0.087704	2.46002E−6

$$P(o_1 = 80|h_1 = 1) = \frac{1}{\sqrt{2\pi\sigma^2_{H=1}}}\exp\left(-\frac{(o_1-\mu_{H=1})^2}{2\sigma^2_{H=1}}\right)$$
$$= \frac{1}{\sqrt{2\pi * 42.25}}\exp\left(-\frac{(80-73.5)^2}{2*42.25}\right) = 0.1012$$
$$P(o_2 = 77|h_2 = 0) = 0.0658$$
$$P(o_3 = 57|h_3 = 0) = 0.0658$$
$$P(o_4 = 67|h_4 = 1) = 0.1012$$

Therefore,

$$P(O|H) = \prod P(o_i|h_i) = 4.43417^{-5}$$

$P(H)$ is decided next. The influence to the energy function exerted by the singleton clique is obtained using Eq. (17). $\zeta(h_i)$ reflects the observation of each node.

$$\varsigma(h_1) = \log(P(o_1|h_1)) = -0.99482$$
$$\varsigma(h_2) = -1.18177;\ \varsigma(h_3) = -1.18177;\ \varsigma(h_4) = -0.99482$$

The influence to the energy function exerted by the neighbor nodes is obtained using Eq. (18). $\xi(h_j,h_i)$ reflects the spatial consistency of the field. $\xi(h_j,h_i)$ has a positive influence to the energy function when h_j and h_i are same, on the other hand, it has a negative influence when h_j and h_i are different. Therefore,

$$\xi(h_2,h_1) = -1;\ \xi(h_4,h_1) = 1;\ \xi(h_1,h_2) = -1;\ \xi(h_3,h_2) = 1;$$
$$\xi(h_2,h_3) = 1;\ \xi(h_4,h_3) = -1;\ \xi(h_1,h_4) = 1;\ \xi(h_3,h_4) = -1;$$

e_{ji} reflects the reliability of local decision made by a neighbor node, node_j, of node_i. Given a hypothesis configuration, the local decision of node_j of node_i is likely equal to the hypothesis of node_i since the nodes close to each other are most likely to have the same event. The reliability of local decision between node_2 and node_1, e_{21}, is true since the local decision of node_2 ($\phi_2 = 1$) is same as the hypothesis of node_1 ($h_1 = 1$). Similarly, the reliabilities of other neighbors are obtained.

$$e_{21} = 1;\ e_{41} = 0;\ e_{12} = 0;\ e_{32} = 1;$$
$$e_{23} = 0;\ e_{43} = 1;\ e_{14} = 1;\ e_{34} = 0;$$

The energy function for hypothesis configuration $H = \{1, 0, 0, 1\}$ is then obtained as:

$$E(H) = \sum_{\{i\}\in C}\alpha_{h_i} - \sum_{\{i\}\in C}\beta\zeta(h_i) - \sum_{\{i,j\}\in C}\delta e_{ji}\xi(h_j,h_i)$$
$$= 0 - \{-0.99482 - 1.18177 - 1.18177 - 0.99482\}$$
$$-\{1^*(-1) + 0^*1 + 0^*(-1) + 1^*1 + 0^*1$$
$$+ 1^*(-1) + 1^*1 + 0^*(-1)\}$$
$$= 4.35318$$

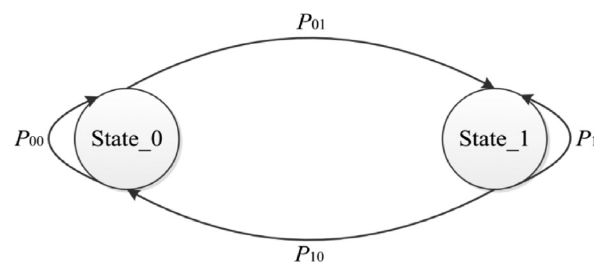

Fig. 6. The two-state Markov process representing a sensor node.

The partition function, Z, can be obtained when summing up the energy functions, and $P(H)$ for $H = \{1, 0, 0, 1\}$ is then calculated.

$$Z = \sum_{h\in H} e^{-E(h)}$$
$$= e^{-0.552084} + e^{-5.972036} + \ldots + e^{-0.552084} = 6.564619$$
$$P(H = h) = Z^{-1}e^{-E(h)} = \frac{e^{-4.353187}}{6.564619} = 0.001959$$

As shown in Table 1, the energy functions for all cases of hypothesis assumption can be obtained using the procedure shown above. With $P(O|H)$ and $P(H)$, $P(H|O)$ is obtained by Eq. (7).

Finally, the hypothesis configuration $H = \{1, 1, 0, 0\}$ of the highest $P(H|O)$ is selected among all the cases as the event occurred. This matches the original observation of the four nodes.

3.2.3. Temporal summarization

The sensor readings collected by a node may present high temporal correlation if the values of its neighbor nodes remain constant or change little. In the process of temporal modeling, Markov chain [22] is employed at the temporal layer to monitor the nodes at spatial layer and detect temporal event. The first-order Markov chain assumes a finite sequence of events over discrete points of time, where the future behavior of the process is based solely on the current state.

A discrete-time Markov chain is a stochastic process which specifies how a random variable changes at discrete points in time. Let ω_t denote a random variable representing the state of a system at time t, where $t = 1, 2, \cdots$ with the Markovian property, namely, given the present state, the future states are independent of it. Let P_{ij} denote the transition probability that the system is in state-j at time (t+1) given the system is in state-i at time t, that is $P_{ij} = P(S_{t+1} = \omega_j \mid S_t = \omega_i)$.

As illustrated in Fig. 6, a two-state Markov model is used to predict the future state of a node, where state_1 represents the

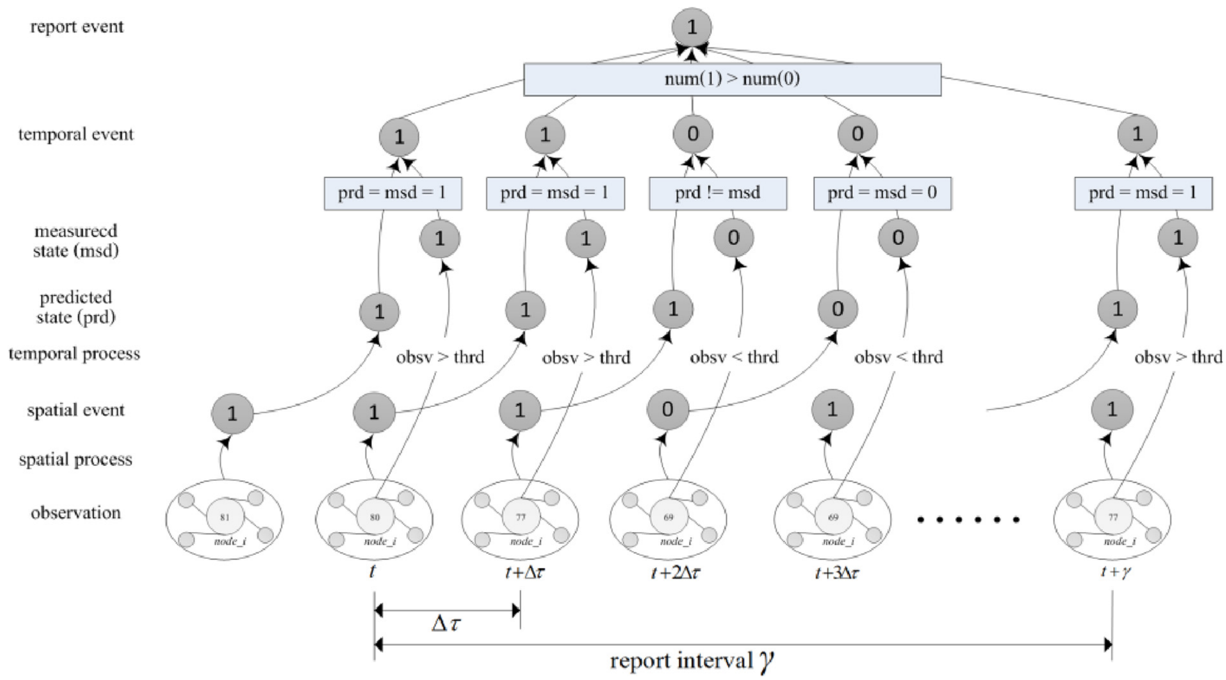

Fig. 7. The process of making a temporal event decision.

detection of an event and state_0 no. Markov model is effective to deal with the problem of modeling of uncertainty and complexity of real world. Here the transition probability between the states can be obtained from the expert views or through a learning process with the training of data. In this paper the transition probabilities are obtained by counting how many times a transition has occurred between any two states normalized by all state transitions in training the data. During the training process described in the next section, measurement noise and channel jitter are injected to the baseline data with Gaussian random variable. Note that a node in state_1 due to the baseline data has a high probability for having a transition to state_1, and the same for the node in state_0.

Deviation from normal behavior for a sensor in time domain is interpreted as temporal event or noise (malfunction of sensor). Noting that noise occurs intermittently, consecutive deviations can be regarded as temporal events. Fig. 7 shows how a node makes an event decision. After identifying the hypothesis configuration, *H*, with the use of MRF on the observations of the sensors during the spatial summarization process, the nodes make binary decision. If its decision is 1, the node is marked as ***S_node***, n_{sp}. A Markov process is individually applied to n_{sp} for a certain amount of time, γ. Let $\triangle\tau$ be the reporting interval. A *temporal event* is decided when the predicted state of n_{sp} through the Markov chain process, $\varpi(n_{sp}, t+\triangle\tau)$, is in accordance with the measured state, $\omega(n_{sp}, t+\triangle\tau)$, and both of them are of state_1. The measured state of a node is obtained by comparing its obserbvation value with the user-specified threshold, e.g., the measured state for *node_i* at time *t* in Fig. 7 is state_1 as its observation is 80 and the threshold is 70. In other words, a node detecting an event occurrence at time *t* through the spatial layer identifies a temporal event only when both the predicted state and measured state indicate an event. The probability of state $\varpi(sp, t+\triangle\tau)$ can be computed by Eq. (23).

$$P(\varpi_t, \ldots, \varpi_{t+\triangle\tau}) = q_{\varpi_t} \prod_{\gamma=t}^{t+\triangle\tau} P_{\varpi_\gamma \varpi_{\gamma+1}} \tag{23}$$

Assume that a temporal event is detected at *t*. However, it may be a false detection caused by errors in the sensors or communication link, or incorrect detection. A spatial event detected by a node may be erroneous due to the noises during communication such as *node_i* at time $(t+2\triangle\tau)$ in Fig. 7. Even though a spatial event is correctly detected with the consideration of the neighbors' decisions, a node itself might be malfunctioning. To deal with such erroneous situation, as shown in Fig. 7, an event is deemed to actually occur only when the number of detections of temporal events is larger than that of no detection during a fixed interval, γ. This approach allows to mitigate the influence of malfunctioning sensor or noise in event detection. Note that only the node detecting temporal event (after spatial event detection) reports the event to the base station.

4. Performance evaluation

In this section computer simulation is conducted to evaluate the performance of the proposed scheme, and its performance is compared with the existing schemes.

4.1. Simulation environment

The simulation is conducted with a network consisting of $N = \{400, 900, 1600, 2500\}$ nodes placed in a square area. The baseline data are generated with a specific distribution of event occurrence. With each sensor reading of baseline data, a positive or negative measurement noise is added. The measurement noise is a Gaussian random variable with the mean of one tenth of the mean value of baseline data, and same variance as the baseline data. Signal jitter is also assumed to occur during data transmission such that the value of the transmitted signal of 1 is switched to 0 and vice versa. The probability of signal jitter is also settable for different simulation runs. The signal strength is assumed to be 0 if fault hypothesis *F* is true or 1 if the alternative hypothesis *T* is true.

The performance metrics adopted in the simulation include the *Precision, Recall, F1-score, Garbage rate*, and *Communication cost*. We define the number of sensor nodes reporting event when actually an event occurs as true positives (*tp*), the number of nodes reporting event when no event actually occurs as false positives (*fp*), and the number of nodes missing actually occurring

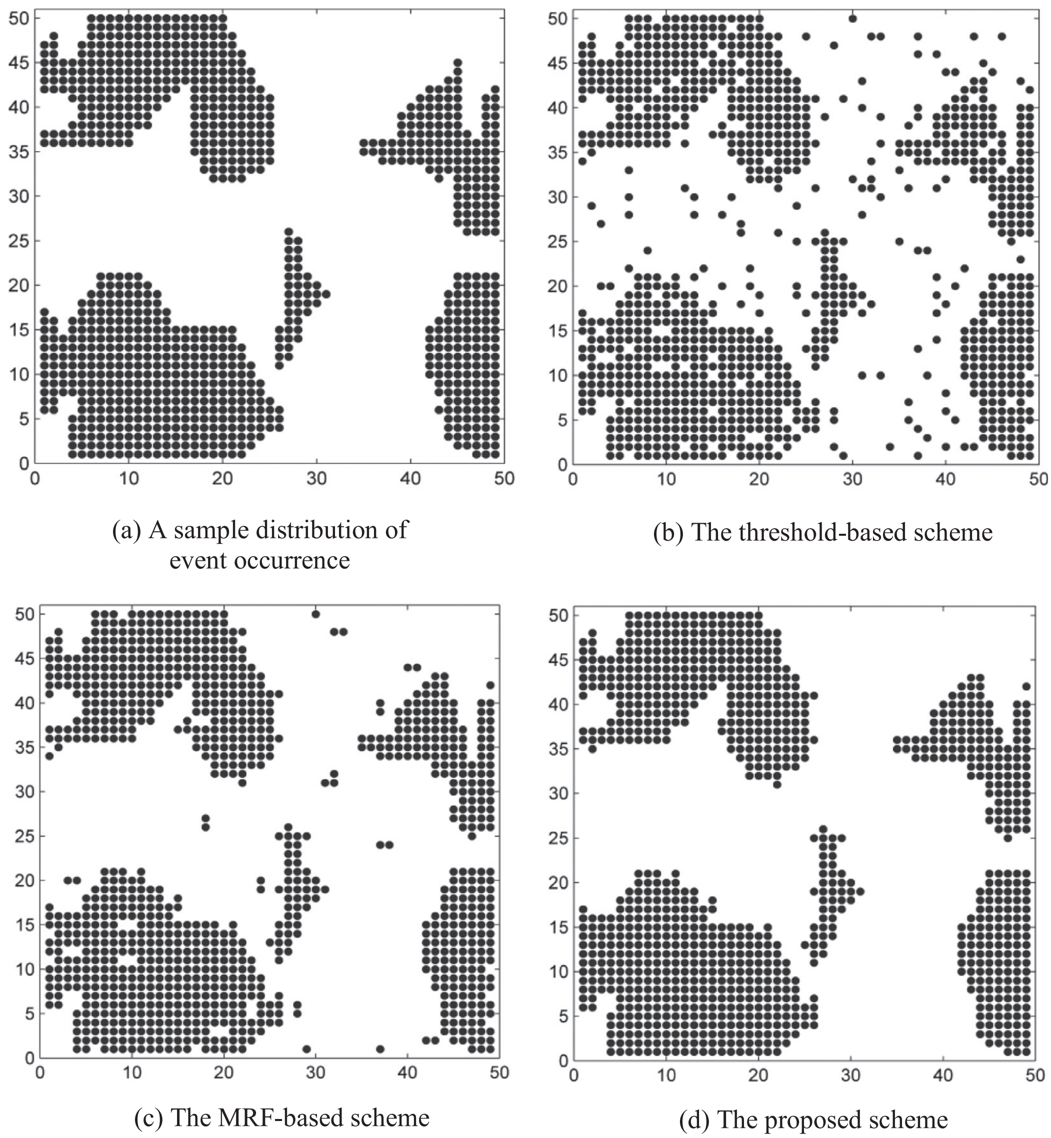

(a) A sample distribution of event occurrence

(b) The threshold-based scheme

(c) The MRF-based scheme

(d) The proposed scheme

Fig. 8. The event detection with 50×50 sensor nodes.

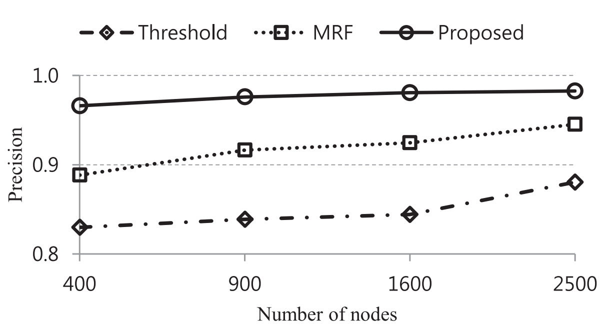

Fig. 9. The comparison of the values of Precision.

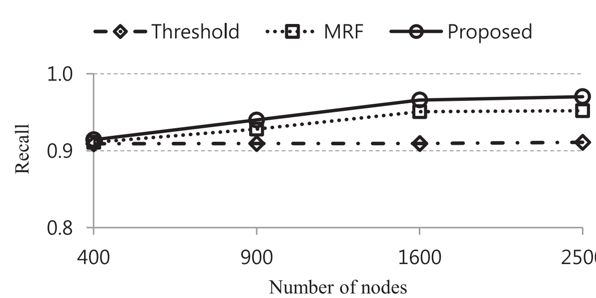

Fig. 10. The comparison of the Recall rates.

event as false negatives (*fn*). *Precision*, obtained by Eq. (24), is the probability to correctly detect an event. *Recall*, defined as Eq. (25), represents the proportion of correctly detected events out of all events occurred. *F1_score* of Eq. (26) is a measure obtained by the harmonic mean of precision and recall. False positives and false negatives deteriorate the performance of an event detection system. Garbage rate, *Grate*, defined as Eq. (27), is the portion of false detection out of entire decisions, used to show the inaccuracy of detection. Eq. (28) represents the communication cost as a log scale in the difference of the number between reported events, N_{rep}, and actually simulated events, N_{act}.

$$Precision = \frac{tp}{tp + fp} \tag{24}$$

$$Recall = \frac{tp}{tp + fn} \tag{25}$$

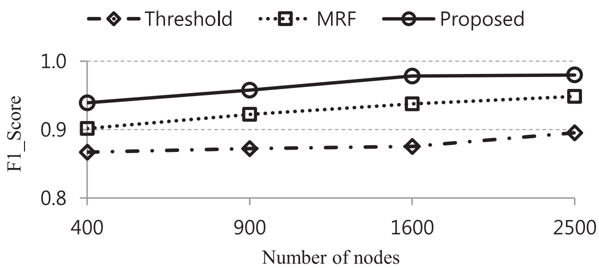

Fig. 11. The comparison of the F1-Score measures.

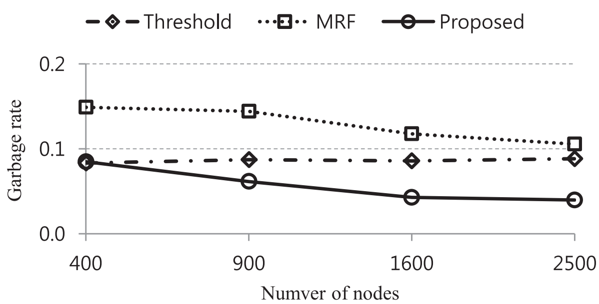

Fig. 12. The comparison of the garbage rates.

$$F1\_score = \frac{2 \times Precision \times Recall}{Precision + Recall} \tag{26}$$

$$Grate = \frac{fp + fn}{tp + fp + fn} \tag{27}$$

$$CommCost = \log_{N_{act}}(N_{rep} - N_{act}) \tag{28}$$

The performance of the proposed approach is compared with the threshold-based scheme which is employed for event detection with typical WSN. It has lowest computational overhead among the existing event detection approaches. The decision is made by comparing the sensor reading with a fixed threshold such that a higher sensor reading than the threshold is considered as the presence of an event. In addition, the learning-based approach is compared, where the MRF is employed without temporal summarization.

4.2. Simulation results

In the first simulation, the failure probabily of each sensor node is set to 0.02. In other words, the measurement noise is added to the sensed data of each node with the probability of 0.02. Based on the sensed data, the decision of each sensor node is 1 if the positive hypothesis T is true, or 0 if the alternative hypothesis F is true. Channel error is also assumed to occur during the transmission of sensor data. The channel randomly encounters signal jitter with the probability of 0.02.

Fig. 8(a) shows an example of event occurrence with 50×50 nodes. When the positive hypothesis is true at a node, it is represented by a dot. Otherwise, the node is not shown in the figure. Different scenarios of simulated events at different time stamps are generated by adding sensor noise and channel jitter. Fig. 8(b)–(d) illustrate the result of event detection with the threshold-based scheme, MRF scheme, and the proposed scheme, respectively. It can be observed that the result of the proposed scheme of Fig. 8(d) is much more close to the original data of Fig. 8(a) than the other schemes.

Fig. 9 compares the precision of event detection of the schemes for different node densities. It can be observed that the precision

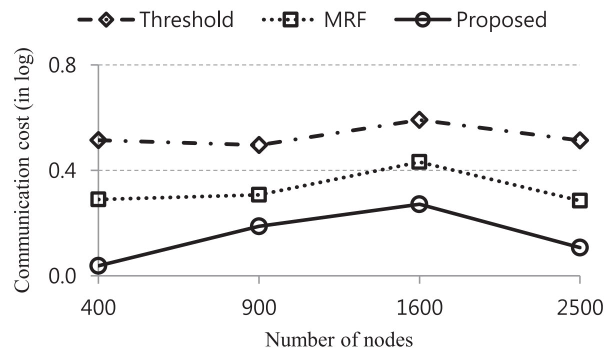

Fig. 13. The comparison of the communication cost.

of the proposed scheme is consistently better than the others. Also, notice that it grows as the network density increases since ***S_node*** is decided after all the neighbors in the same clique are considered using the fusion function. In contrast, the simple threshold scheme reports an event without taking the decision of neighor nodes into account. Similarly, missing the consideration of the temporal correlation between the sensor reading of the nodes, the MRF-based approach shows lower precision than the proposed approach since it lacks the filtering of bursty error readings. The simulation results verify that considering both spatial and temporal in an integrated way substantially improves the detection precision.

Fig. 10 shows the comparison of Recall rates of the schemes. Note that the proposed scheme decides *S_node* considering the data of neighboring nodes and uses Markov model to predict if an event has been detected in the *S_node* or not in a period of time. In contrast, the threshold approach reports an event just based on the currently sensed data, and thus event detection is made by the condition of individual nodes independently.

In order to comprehensively investigate the performances of the schemes, a weighted measure, F1_Score, is considered which integrates the precision and recall rate. Fig. 11 demonstrates the merit of the proposed scheme compared with the other schemes in terms of the F1_Score measure. Obviously, the proposed scheme outperforms the others, and the measure increases as the network density becomes higher since the spatial correlation between the observations is higher. It is deemed that the proposed scheme can detect events with a higher accuracy and efficiency using WSN.

Fig. 12 shows the comparison of the garbage rates, indicating how false positive and false negative events degrade the performance of the schemes. Observe from the figure that the garbage rate of the proposed scheme is consistantly lower than the other two schemes.

The communication cost is measured by the log scale of the difference in the number of reported events and actually simulated events. As can be seen from Fig. 13, the proposed scheme always requires lower communication cost than the others.

In the second simulation the performance of the schemes are evaluated by varying both the sensor noise probability and channel jitter probability from 0.02 to 0.2 to check the influence of them to the performance. A new performance criterion called *Efficiency* is adopted here, which is *F1_Score/Grate*. Observe from Fig. 14 that the *Efficiency* decreases as the sensor failure and channel error probability increase. Observe that the proposed scheme shows the best *Efficiency* among the three schemes for the given sensor failure probability and channel error probability, as much as 2.4 and 7.5 times larger than the threshold and MRF-based scheme, respectively. Also, notice that the channel jitter imposes larger impact to the performance than sensor noise. This is because sensor noise can be compensated by spatial summarization but channel jitter

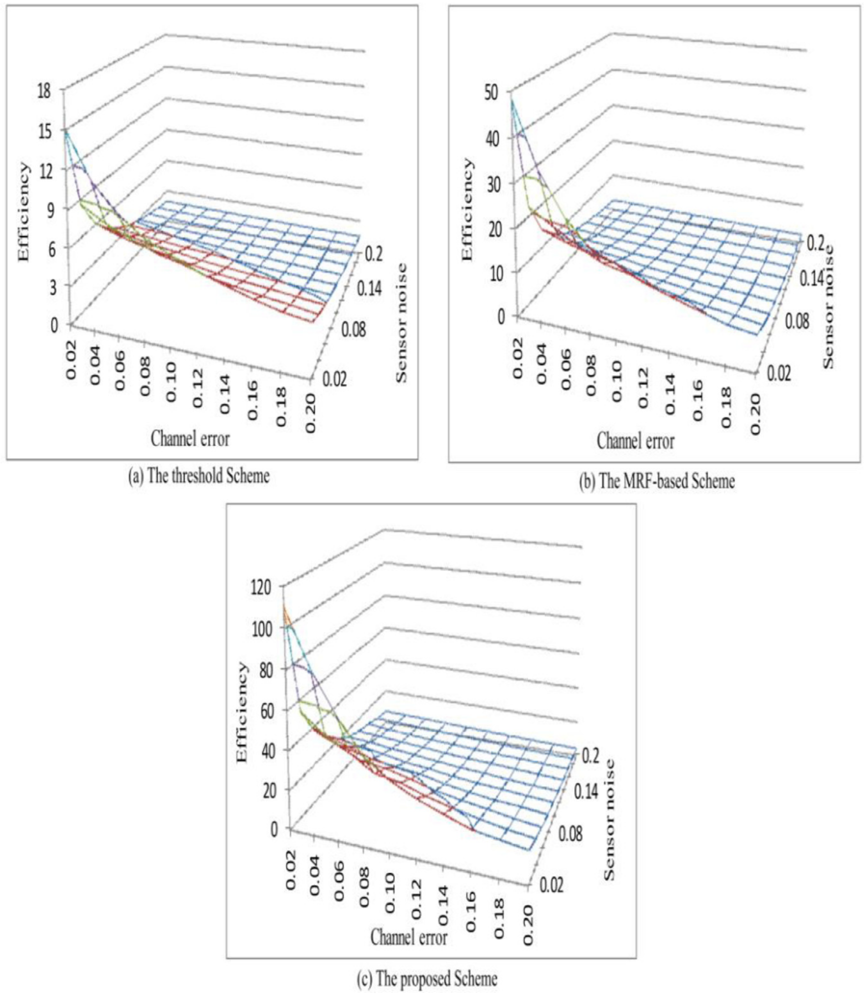

Fig. 14. The comparison of *Efficiency*.

can switch a true positive hypothesis to a false positive hypothesis or vice versa.

5. Conclusion

In this paper we have presented a novel event detection approach considering the properties of both spatial and temporal relationship in wireless sensor network. In order to increase the detection accuracy, the proposed scheme integrates spatial event detection and temporal event detection using a hierarchical structure of sensor nodes. In addition, a fusion rule considering the weight of the sensor and spatial information was employed with MRF to fuse the decisions of the sensor nodes along with the Markov chain model for temporal analysis. Computer simulation revealed that the proposed scheme significantly improves the detection accuracy and communication overhead compared with the threshold approach and MRF-based event detection approach.

Energy consumption is a crucial issue for WSN since the deployed sensor nodes have limited battery power. Continuous sensing and data transmission will consume large energy, which shortens the lifetime of the nodes. The proposed scheme will be improved by controlling the node operation based on the sleep-and-wakeup mechanism for energy efficiency. In addition, the mechanism for systematically determining the operation parameters required in the proposed event detection scheme will be investigated in the future. The event detection scheme with insufficient number of nodes in the target area is also important. The correlation between the spatial and temporal data needs to be handled in an integrated way. A new approach will also be researched to compare the effectiveness of different ways of integration of them.

Acknowledgment

This research was supported by the second Brain Korea 21 PLUS project and MSIP (Ministry of Science, ICT & Future Planning), Korea in the ICT R&D program of MSIP/IITP(B0717-16-0070), and Samsung Electronics (S-2014-0700-000).

References

[1] M.A. Mahmood, W.K.G. Seah, I. Welch, Reliability in wireless sensor networks: a survey and challenges ahead, Comput. Netw. 79 (2015) 166–187 January 2015.
[2] Y. Li, L.E. Parker, Nearest neighbor imputation using spatial–temporal correlations in wireless sensor networks, Inform. Fusion 15 (2014) 64–79 January 2014.
[3] T.Y. Wang, Q. Cheng, Collaborative event-region and boundary-region detections in wireless sensor networks, IEEE Trans. Signal Process 56 (6) (June 2008) 2547–2561.
[4] A. Mousavi, M. Duckhem, R. Kotagiri, A. Rajabifard, Spatio-temporal event detection using probabilistic graphical models (PGMs), in: Proceedings of IEEE Symp. Computational Intelligence and Data Mining (CIDM), Singapore, April 2013, pp. 81–88.
[5] S. Li, Y. Lin, S.H. Son, J.A. Stankovic, Y. Wei, Event detection services using data service middleware in distributed sensor networks, Telecommun. Syst. 26 (2-4) (June 2004) 351–368.
[6] M. Collotta, L.L. Bello, G. Pau, A novel approach for dynamic traffic lights management based on wireless sensor networks and multiple fuzzy logic controllers, Expert Syst. Appl. 42 (13) (August 2015) 5403–5415.

[7] K.X. Thuc, K. Insoo, A collaborative event detection scheme using fuzzy logic in clustered wireless sensor networks, AEU-Int. J. Electron. Commun. 65 (5) (May 2011) 485–488.
[8] K. Kapitanova, S.H. Son, K.D. Kang, Using fuzzy logic for robust event detection in wireless sensor networks, Ad Hoc Netw. 10 (4) (June 2012) 709–722.
[9] W. Xue, Q. Luo, H.K. Pung, Modeling and detecting events for sensor networks, Inform. Fusion 12 (3) (July 2011) 176–186.
[10] X. Pei, X. Chen, K.T. Kim, S.W. Kim, H.Y. Youn, Spatio-temporal event detection: a hierarchy based approach for wireless sensor network, in: Proceedings of IEEE International Conference on Cyber-Enabled Distributed Computing and Knowledge Discovery (CyberC 2014), Shanghai, October 2014, pp. 372–379.
[11] W. Xue, Q. Luo, H. Wu, Pattern-based event detection in sensor networks, Distrib. Parallel Dat. 30 (1) (February 2012) 27–62.
[12] W. Xue, Q. Luo, L. Chen, Y. Liu, Contour map matching for event detection in sensor networks, in: Proceedings of international conference on Management of data (ACM SIGMOD), Chicago, June 2006, pp. 145–156.
[13] G. Wittenburg, N. Dziengel, C. Wartenburger, J. Schiller, A system for distributed event detection in wireless sensor networks, in: Proceedings of the 9th ACM/IEEE International Conference on Information Processing in Sensor Networks, Stockholm, April 2010, pp. 94–104.
[14] M. Bahrepour, Y. Zhang, N. Meratnia, P.J.M. Havinga, Use of event detection approaches for outlier detection in wireless sensor networks, in: Proceedings of 5th International Conference on Sensor Networks and Information (ISSNIP), Melbourne, December 2009, pp. 439–444.
[15] Y. Singh, S. Saha, U. Chugh, C. Gupta, Distributed event detection in wireless sensor networks for forest fires, in: Proceedigns of 15th International Conference on Computer Modelling and Simulation (UKSim), Cambridge, April 2013, pp. 634–639.
[16] T.Y. Wang, M.H. Yang, J.Y. Wu, A sliding window approach for dynamic event-region detection in sensor networks, in: Proceeding of International Conference on Information Science, Electronics and Electrica Engineering (ISEEE), Sapporo, April 2014, pp. 2025–2028.
[17] J. Yin, D.H. Hu, Q. Yang, Spatio-temporal event detection using dynamic conditional random fields, in: Proceedings of International Joint Conference on Artificial Intelligence (IJCAI), California, July 2009, pp. 1321–1326.
[18] Y.C. Wang, Y.Y. Hsieh, Y.C. Tseng, Multiresolution spatial and temporal coding in a wireless sensor network for long-term monitoring applications, IEEE Trans. Comput. 58 (6) (January 2009) 827–838.
[19] S.Z. Li, Markov random field modeling in image analysis, 3th edition, New York, USA: Springer-Verlag, 2009.
[20] T. Wu, Q. Cheng, Adaptive Bandwidth Allocation for Dynamic Event Region Detection in Wireless Sensor Networks, IEEE Trans. Wireless Commun. 13 (9) (September 2014) 5107–5119.
[21] T.Y. Wang, C.T. Yu, Collaborative event region detection in wireless sensor networks using Markov random fields, in: Proceedings of 2nd International Symposium on Wireless Communication Systems, Siena, September 2005, pp. 493–497.
[22] S.P. Meyn, R.L. Tweedie, Markov chains and stochastic stability, 2nd edition, Cambridge University Press, UK, 2009.

Xianda Chen received the BS degree in Software Engineering from Northwestern Polytechnical University, Xi'an, China, in 2013, and the Master degree in Electrical and Computer Engineering from Sungkyunkwan University, Suwon, Korea, in 2015. He has published two papers in int'l journals and three in IEEE Int'l conference proceedings. His current research interests include the next generation of mobile communication and wireless sensor networks.

Kyung Tae Kim received the BS and MS degree in Computer Science and Engineering from Suwon University and Sungkyunkwan University, Suwon, Korea, in 2003 and 2005, respectively, and the PhD degree in computer engineering from the Sungkyunkwan University, in 2013. He is presently research staff of College of Information and Communication Engineering, Sungkyunkwan University, Suwon, Korea, and Director of Ubiquitous computing Technology Research Institute. He served as the Financial Co-chairs of the International Conference on Cyber-enabled Distributed Computing and Knowledge Discovery, 2015. He has also been directing several projects funded by Korean government including the mobile sensor networks. He has published more than 60 papers in int'l journals and conference proceedings. His research interests include distributed and ubiquitous computing, system software and middleware, big data processing, and sensor networks.

Hee Yong Youn received the BS and MS degree in electrical engineering from Seoul National University, Seoul, Korea, in 1977 and 1979, respectively, and the PhD degree in computer engineering from the University of Massachusetts at Amherst, in 1988. He had been Associate Professor of Department of Computer Science and Engineering, The University of Texas at Arlington until 1999. He is presently Professor of College of Software, Sungkyunkwan University, Suwon, Korea, and Director of Ubiquitous computing Technology Research Institute. He is also Consulting Professor of Software R&D Center, Device Solutions, Samsung Electronics, Korea. His research interests include distributed and ubiquitous computing, IoT, and intelligent system. He has published more than 400 papers in int'l journals and conference proceedings, and received Outstanding Paper Award from the 1988 IEEE International Conference on Distributed Computing Systems, 1992 Supercomputing, and 2012 IEEE Int'l Conf. on Computer, Information and Telecommunication Systems, 2014 The 6th International Conference on Cyber-Enabled Distributed Computing and Knowledge Discovery, respectively. Dr. Youn has also been General Chair of IEEE PRDC 2001, Int'l Conf. on Ubiquitous Computing Systems (UCS) in 2006 and 2009, UbiComp 2008, CyberC 2010, Program Chair of PDCS 2003 and UCS 2007. Dr. Youn is a senior member of the IEEE Computer Society.